Journal of Molecular and Cellular Cardiology 127 (2019) 67–73

Contents lists available at ScienceDirect

Journal of Molecular and Cellular Cardiology

journal homepage: www.elsevier.com/locate/yjmcc

ERK mediated survival signaling is dependent on the Gq-G-protein coupled receptor type and subcellular localization in adult cardiac myocytes

Erika F. Dahl[a], Steven C. Wu[b], Chastity L. Healy[b], Jocelyn Perry[b], Timothy D. O'Connell[a,b,*]

[a] Department of Pharmacology, University of Minnesota, MN 55455, USA
[b] Department of Integrative Biology and Physiology, University of Minnesota, MN 55455, USA

ARTICLE INFO

Keywords:
Cell signaling
Fluorescent lifetime imaging microscopy
ERK
Cardiac myocytes
α1-adrenergic receptors
Angiotensin receptors

ABSTRACT

G protein-coupled receptors that signal through Gαq (GqPCRs), like α1-adrenergic and angiotensin receptors (α1-AR, AT-R), are traditionally thought to mediate pathologic remodeling in heart failure, including cardiac myocyte death. However, we previously demonstrated that α1- ARs are cardioprotective and identified an α1A-subtype-ERK survival-signaling pathway in adult cardiac myocytes. Recently, we demonstrated that α1-ARs localize to and signal from the nucleus, whereas AT-R localize to and signal from the sarcolemma in adult cardiac myocytes. Thus, we proposed a novel paradigm, predicated on compartmentalization of GqPCR signaling, to explain the phenotypic diversity of GqPCRs. Here, we tested the hypothesis that differential subcellular compartmentalization of α1-AR and AT-R mediated activation of ERK might explain the differential effects of these receptors on cardiac myocyte survival. Using a fluorescent ERK activity FRET-based biosensor, EKAR, to measure subcellular localization and extent of receptor-mediated ERK activation in single adult cardiac myocytes, we found that α1-ARs induced ERK activity at the nucleus and in the cytosol in 60% of cardiac myocytes, whereas AT-Rs showed no consistent ERK activation. The cell-specific α1-mediated activation of ERK in 60% of adult cardiac myocytes showed concordance with previous studies indicating that the α1A-subtype is expressed in only 60% of cardiac myocytes. Consistent with the ability to activate ERK, we found that only α1-ARs induced phosphorylation of Bcl-2 family member Bad, improved mitochondrial membrane stability, and promoted cardiac myocyte survival. In summary, our results suggest that compartmentalization of GqPCRs dictate activation of ERK and cardiac myocyte survival in adult cardiac myocytes.

1. Introduction

The established model of cardiac Gq-coupled G-protein coupled receptor (GqPCR) signaling is that GqPCR signaling worsens heart failure. In support of this model, overexpression of Gαq in cultured cardiac myocytes induces hypertrophy with re-expression of fetal genes typically associated with pathologic ventricular remodeling, while overexpression of a constitutively active Gαq induces apoptosis [1]. In mice, four- or five-fold cardiac myocyte-specific overexpression of Gαq induces pathologic hypertrophy, while eight-fold overexpression of Gαq induces cardiac myocyte apoptosis, heart failure, and death by 11 weeks [1]. Further, cardiac myocyte-specific deletion of Gq/G11 or overexpression of a Gq-inhibitory peptide prevents pathologic remodeling in a model of pressure overload induced hypertrophy [2,3].

Angiotensin receptors (AT-R) are prototypical cardiac GqPCRs that induce cardiac myocyte death [4] and pathologic ventricular remodeling [5–7]. Clinically, angiotensin receptor blockers and angiotensin converting enzyme inhibitors are both used in heart failure, in part due to their direct effects on cardiac myocytes [8]. In contrast, α1-adrenergic receptors (α1-AR) do not conform to this model of maladaptive GqPCR signaling [9]. In mice, α1-ARs are required for physiologic postnatal hypertrophy and an adaptive response to pathologic stress [10–13]. In cardiac myocytes, we identified an α1A-subtype-ERK survival signaling pathway, the absence of which helps explain the

Abbreviations: α1-AR, α1-adrenergic receptors; α1AKO, α1A-AR knockout; α1BKO, α1B-AR knockout; α1ABKO, α1A-AR and α1B-AR double knockout; AMVM, adult mouse ventricular myocytes; AngII, angiotensin II; AT-R, angiotensin receptor; β1-AR, β1-adrenergic receptor; Dox, doxorubicin; EKAR, extracellular kinase activity reporter; FLIM, fluorescent lifetime imaging microscopy; FRET, Förster resonance energy transfer; GqPCR, Gq coupled G-protein coupled receptor; HDAC, histone deacetylase; IRF, instrument response function; PE, phenylephrine; P-Bad, phosphorylated Bad; P-ERK, phosphorylated ERK; PLCβ1, Phospholipase C β1; T-ERK, total ERK

* Corresponding author at: Department of Integrative Biology and Physiology, The University of Minnesota, 2231 6th St SE, Cancer and Cardiovascular Research Building, 3-141, Minneapolis, MN 55455, USA.
E-mail address: tdoconne@umn.edu (T.D. O'Connell).

https://doi.org/10.1016/j.yjmcc.2018.11.020
Received 9 October 2018; Accepted 29 November 2018
Available online 04 December 2018
0022-2828/

maladaptive response to pathologic stress in mice lacking cardiac α1-ARs [14]. Clinically, α1-AR antagonists worsen outcomes in hypertension and heart failure [9]. Together, these findings suggest that GqPCR signaling is more complex than the traditional model of GqPCR maladaptive signaling.

Recently, we proposed that differential subcellular compartmentalization of Gq-PCRs might explain differences in GqPCR physiologic function [15]. Specifically, we demonstrated that α1-ARs localize to and activate phospholipase Cβ1 (PLCβ1) at the nucleus while AT-Rs primarily localize to and activate PLCβ1 at the sarcolemma in adult cardiac myocytes. This differential subcellular compartmentalization of α1-AR and AT-R signaling produced differential activation of histone deacytlase (HDAC)-nuclear export and hypertrophic transcriptomes correlating with cardioprotective α1-signaling and maladaptive AT-R signaling.

With consideration towards our new model of compartmentalized GqPCR signaling, we hypothesized that differential subcellular compartmentalization of α1-AR and AT-R mediated activation of ERK might explain the differential effects of these receptors on cardiac myocyte survival. Using a Förster resonance energy transfer (FRET)-based biosensor that measures ERK activity, extracellular signal-regulated kinase activity reporter (EKAR) [16], we measured both the compartmentalization and degree of α1-AR and AT-R mediated activation of ERK in adult cardiac myocytes. Briefly, we found that α1-ARs activated ERK at the nucleus and the cytosol in a subset of cardiac myocytes consistent with known expression patterns of the α1A-subtype, whereas AT-Rs showed no consistent activation of ERK. Further, we found that α1-ARs, but not AT-Rs, induced phosphorylation of Bcl-2 family member Bad, improved mitochondrial membrane stability, and promoted cardiac myocyte survival. Finally, we identified clear differences in compartmentalization of α1-AR and AT-R mediated activation of ERK, consistent with respective ability or inability of these receptors to promote cell survival.

2. Materials and methods

2.1. Adult mouse ventricular myocytes (AMVM)

AMVM were isolated and cultured as previously described from male and female 10–15 week old, C57BL/6 J mice [17].

2.2. Western blotting and analysis

Cardiac myocytes were plated on 35 mm laminin coated dishes and cultured for 24 h. To activate ERK, myocytes were treated for 5 min at 37 °C with vehicle, phenylephrine (PE, 20 μM) or angiotensin II (AngII, 100 nM), and harvested in 2× Laemmli sample buffer. To activate Bad, myocytes were treated for 15 min at 37 °C with vehicle, doxorubicin (Dox, 2 μM), PE (20 μM), or AngII (100 nM), and harvested in 2× Laemmli sample buffer. Equivalent number of cells were loaded per lane. Western blots were performed with primary antibodies to phosphorylated p44/42 MAPK (1:500, Cell Signaling) and total p44/42 MAPK (1:500, Cell Signaling), anti-Bad (phospho S112) (1:500, Abcam), anti-Bad (1:2000, Abcam), and secondary antibody conjugated to HRP (1:5000, Cell Signaling). Densitometry was performed using Image Lab software (Bio-Rad). Data are presented as the percent contribution of each treatment (vehicle control, Dox, PE, AngII) to the phosphorylated ERK and Bad signal, respectively. Values are expressed as mean ± SEM. Data were analyzed by one-way ANOVA, and $P < 0.05$ was considered significant.

2.3. Extracellular signal-regulated kinase activity reporter (EKAR)

The cytoplasmic EKAR plasmid was a gift from Karel Svoboda (Addgene, #18679). EKAR consists of the Cerulean and Venus FRET pair, a substrate phosphorylation peptide, Thr48 from Cdc25, and a phospho-binding domain. ERK activation induces phosphorylation of EKAR leading to increased FRET (FRET-on) [16] (Fig. 2A). An adenovirus expressing EKAR was generated with the AdEasy System (Agilent).

2.4. Fluorescence lifetime imaging microscopy (FLIM) and analysis of EKAR activity

Cardiac myocytes were plated on laminin-coated glass coverslips in a 14 mm microwell within 35 mm petri dishes (MatTek), infected with EKAR adenovirus (multiplicity of infection 250), and cultured for 40 h at 37 °C. Myocytes expressing EKAR were identified by 512 × 512 pixel, 1 msec linescan with the excitation of Cerulean at 433 nm and emission at 475 nm. EKAR activity was recorded in a control cell and then in a separate treated cell (PE or AngII) from the same dish, due to myocyte death from phototoxicity caused by prolonged laser stimulation during live-cell FLIM, and the tendency of myocytes to contract spontaneously and move out of focus. Myocytes were treated with either 20 μM PE, 100 nM AngII, or 100 nM A61603 (Sigma Aldrich), at 25 °C for 5 min. In some experiments, myocytes were pre-treated with vehicle (DMSO) or the MEK1 inhibitor PD98095 (100 nM) for one hour at 37 °C prior to PE treatment.

All data was collected on an Olympus FluoView FV1000 IX2 Inverted Confocal Microscope with PicoQuant 405 pulsed laser (80 MHz) at 60× magnification (oil immersion). On average, 1×10^7 photons were collected per cell on SPCM software (Becker & Hickl).

Data were analyzed using FLIMFit software (Imperial College London) using the time-domain fluorescence lifetime algorithm for production of intensity images, which are displayed as a color gradient (blue-red), with red indicating regions of highest EKAR activity. [18]. Data were calculated by setting the instrumental response function (IRF) to time zero which was assumed to be the peak of the IRF by manipulating the time minimum under the IRF tab [18]. Images were fit using the following settings: pixel-wise global fitting, global binning, 2-exponential decay components, global fitting, and variable projection.

Quantitatively, raw intensity values for each cell were determined and standardized to the number of photons collected. Raw intensity values for treated versus control were analyzed using both unpaired and paired *t*-tests. The limitations of phototoxicity and movement of contracting myocytes over time influenced our decision to use a paired analysis of control and treated cell from the same dish. However, we also considered all data in an unpaired analysis.

Interestingly, intensity was not increased uniformly in all treated myocytes, suggesting a group of 'responders' and 'non-responders,' which was further analyzed. For the paired analysis, we calculated the intensity ratio of treated/control for each myocyte pair, and 'responders' were defined by an intensity ratio of > 1 and 'non-responders' defined as having a ratio of < 1, and differences were calculated using a paired *t*-test. For the unpaired analysis, for each myocyte we calculated the intensity ratio of (treated intensity)/(average control intensity), and 'responders' were defined by having an intensity ratio > 1, whereas non-responders were defined as having a ratio of < 1, and differences were calculated using a one-sample *t*-test, which evaluates confidence intervals versus a reference value (1.0 in this case). Ultimately, both data analyses produced similar results, and we present the results of each analysis (Table 1).

All values are expressed as mean ± SEM. Data were analyzed by a paired, two-tailed student's *t*-test (treated vs control) or unpaired student's t-test as indicated and presented as fold-change using Prism 6.0 (GraphPad Software, Inc.) and $P < 0.05$ was considered significant.

2.5. JC-1 mitochondrial membrane potential assay

Cardiac myocytes were plated on 35 mm laminin coated dishes, cultured for 24 h, and treated for 2 h at 37 °C with either vehicle, Dox

(2 μM), PE (20 μM,) or AngII (100 nM). After 2 h, myocytes were loaded with 5 μM JC-1 (ThermoFisher) for 30 min at 37 °C, and after 30 min the medium containing JC-1 was aspirated and replaced with fresh, dye-free medium. All data was collected on an Olympus FluoView FV1000 IX2 Inverted Confocal Microscope using a 10× objective (air) and the AF594 filter set. Three images per treatment dish were collected, and fluorescence intensity and rod-round count were determined using FIJI. Values are expressed as mean ± SEM. Data were analyzed by one-way ANOVA, and $P < 0.05$ was considered significant.

3. Results

3.1. α1-ARs, but not AT-Rs, rapidly activate ERK in adult cardiac myocytes

Based on the differential outcomes of activated α1-ARs and AT-Rs on cardiac myocyte survival, we sought to determine if GqPCR activation of ERK correlated with their survival. Here, we measured global ERK activity in cultured adult cardiac myocytes, by treating AMVM with either the α1-AR agonist PE or the AT-R agonist AngII and measuring ERK phosphorylation at Thr202/Tyr204 as a marker of ERK activation. As expected, PE increased the activation of ERK, whereas AngII had no significant effect (Fig. 1A–B).

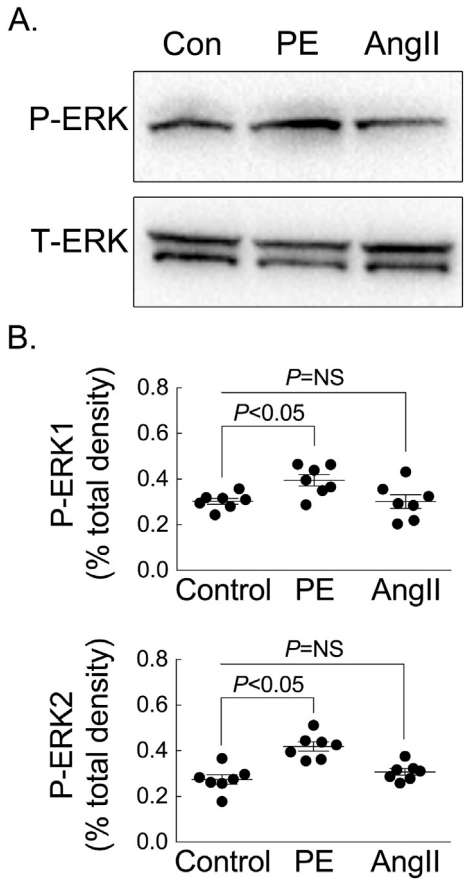

Fig. 1. α1-ARs, but not AT-Rs, rapidly activate ERK in adult cardiac myocytes. A. *ERK Western blot.* WT AMVM were treated with vehicle (Con), phenylephrine (PE, 20 μM), or angiotensin II (AngII, 100 nM) for 5 min. Western blots were performed with primary antibodies to phosphorylated ERK (PERK (Thr202/Tyr204), top) or total ERK (TERK, bottom). B. *Quantification of ERK phosphorylation.* Densitometry presented as percent of each treatment to the phosphorylated ERK1 or ERK2 signal for n = 7 different cultures. Data are presented as Mean ± SEM, and were analyzed by one-way ANOVA ($P = 0.002$ for the primary interaction) with a Tukey post-test, where $P < 0.05$ was considered significant.

3.2. α1-ARs activate ERK at the nucleus and in the cytosol in a subset of adult cardiac myocytes

Western blots provide only a one-dimensional readout of ERK activation in a population of cells or tissue, but provide no insight into degree or localized, intracellular kinase activity. To address this, we employed a fluorescent biosensor of ERK activity, EKAR [16], to compare α1-AR and AT-R mediated activation of ERK (Fig. 2A). EKAR detects kinase activity through phosphorylation of an ERK target site, a peptide containing a known ERK phosphorylation site, Thr48 from Cdc25, which results in an increased EKAR FRET signal. EKAR FRET activity was detected by FLIM, which measures changes in the lifetime decay between the inactive and active state of the fluorophore donor, Cerulean. Further, FLIM is independent of probe concentration, which can vary between cells, and eliminates control measurements of donor and acceptor fluorescence.

In adult cardiac myocytes expressing EKAR, verified by Cerulean fluorescence, PE increased EKAR activity, detected by an increase in intensity at or near the nucleus as well as the cytosol (Fig. 2B–C). Intensity is a calculation of the proportion of Cerulean in the active state and is displayed graphically on a generated image of the myocyte with the sites of highest EKAR activity indicated in red. In addition, fold-changes in EKAR intensity for treated versus control myocytes were calculated by both paired analysis and unpaired analysis as described in the methods section. PE demonstrated a similar trend to increase global EKAR intensity in both paired and unpaired analyses (Table 1, Fig. 2D, paired analysis). Qualitatively, this result agrees with the Western blot analysis, but it should be noted that the PE-induced increase in EKAR intensity signal was very small due to the fact that we measured intensity for the entire myocyte, but observed ERK activated in a specific area of of the myocyte. This indicates a low signal to background ratio, but focusing only on the activated areas would bias us towards a positive response. However, we emphasize that the purpose of this experiment was not necessarily to ascertain *whether* ERK was activated, but rather *where* ERK was activated and in *what proportion* of cells, essentially the goal of our FLIM analysis.

Interestingly, during our analysis, we observed that not all PE-treated myocytes exhibited an increase in EKAR intensity (Fig. 2E). Upon further analysis, we classified PE-treated myocytes as responders and non-responders, and again fold-changes in EKAR intensity for treated versus control myocytes were calculated by both paired analysis and unpaired analyses as described in the methods section. For both analyses, we identified 13/21 (62%) myocytes as responders and 8/21 (38%) as non-responders. In responders, PE significantly increased EKAR intensity in both paired and unpaired analyses (Table 1, Fig. 2F, paired analysis), in agreement with the Western blot analysis. Conversely, in non-responders, PE significantly reduced EKAR intensity in both paired and unpaired analyses (Table 1, Fig. 2G, paired analysis), although the functional significance of this decrease is unclear at this time. A potential confounding effect would be if control intensity differed between responder and non-responder myocytes, but this was not the case for myocytes based on the paired analysis (Table 1). To confirm the PE-mediated activation of EKAR was indeed due to activation of ERK, we performed experiments using the MEK1 inhibitor PD98095 (Supplemental Fig. 1). We observed again that PE increased EKAR intensity, which was inhibited by PD980095, suggesting that the increase in EKAR intensity was secondary to activation of ERK. Furthermore, we observed similar trends towards α1-mediated increased EKAR intensity with the α1A-subtype-specific ligand A61603 in adult cardiac myocytes, but no response in α1ABKO adult cardiac myocytes that lack α1-ARs, confirming specificity for α1-mediated activation of EKAR (Supplemental Fig. 2). In summary, α1-AR stimulation activated ERK in 62% of adult cardiac myocytes (Fig. 2H), which shows good concordance with previous reports indicating that the α1A-subtype, the primary subtype associated with activation of ERK [14], is expressed in only 60% of adult cardiac myocytes [19].

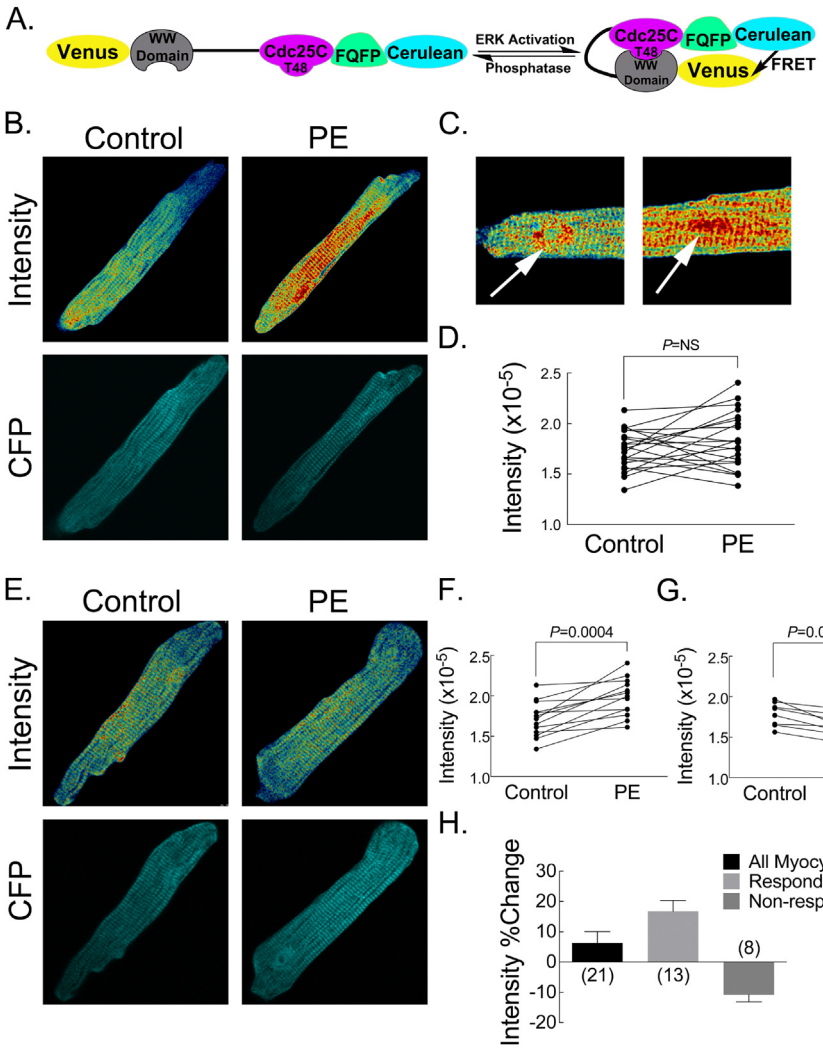

Fig. 2. α1-ARs activate ERK at the nucleus and in the cytosol in a subset of adult cardiac myocytes.
A. *Schematic of EKAR.* Modified from Harvey et al. [16]. B. *α1-AR-induced activation of EKAR in adult cardiac myocytes.* Myocytes expressing EKAR were detected by Cerulean fluorescence (CFP, bottom images) and treated with vehicle (Control) or phenylephrine (PE, 20 μM) for 5 min at 25 °C. EKAR activity was recorded by FLIM and intensity images were generated with red indicating increased EKAR activity (top images) as described in detail in the Methods. C. *α1-AR induced EKAR activity at the nuclei in adult cardiac myocytes.* Intensity images from PE-treated myocytes showing increased EKAR at the nuclei, indicated by the arrows. D. *EKAR intensity.* EKAR intensity, corrected for photons collected, for control (n = 21) and PE treated myocytes (n = 21). Individual myocytes are shown, and paired groups are indicated. Average intensity for control versus PE treated myocytes were compared by paired (shown, Table 1) and unpaired *t*-test (Table 1). E. *α1-ARs do not activate EKAR in all adult cardiac myocytes.* As in (B) myocytes were treated with vehicle (Control) or PE and intensity images were generated. As shown, not all myocytes demonstrated increased EKAR activity in response to PE treatment. F, G. *EKAR intensity; Grouping of PE-treated myocytes as responders (F) and non-responders (G).* As described in the Methods, we grouped PE-treated myocytes into responder (n = 13) and non-responder (n = 8) groups based on EKAR intensity. Average intensity for control versus PE treated myocyte responders (F) and non-responders (G) were each compared by paired (shown, Table 1) and unpaired t-test (Table 1) as described in the Methods. H. *Average fold-change in EKAR.* Average fold change in intensity for all myocytes, responders, and non-responders was calculated using a paired (shown) and unpaired analysis (Table 1).

3.3. AT-Rs do not significantly activate ERK in adult cardiac myocytes

In adult cardiac myocytes expressing EKAR, verified by cerulean fluorescence, AngII failed to produce a consistent increase in EKAR activity (Fig. 3A–B). Furthermore, AngII failed to change global EKAR intensity in both paired and unpaired analyses (Table 1, Fig. 3B, paired analysis). Similar to PE, we observed that AngII possibly increased EKAR activity in a subset of cardiac myocytes (9/22 myocytes, paired analysis, 8/22 myocytes unpaired analysis). Interestingly, in the potential AngII responder myocytes, we failed to observe EKAR activity at the nuclei. However, AngII mediated activation of ERK in the identified subset of myocytes was tempered by a significant difference observed in baseline intensity in responders versus the non-responders in the paired analysis that would tend to negate the potential differences in EKAR activity (Table 1). Therefore, we concluded that AngII had no net significant effect on ERK activation in adult cardiac myocytes, agreeing with the results of our Western blot analysis (Fig. 1).

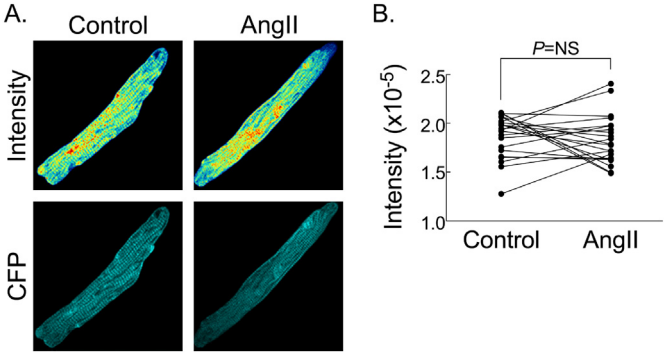

Fig. 3. AT-Rs do not significantly activate ERK in adult cardiac myocytes.
A. *AT-R-induced activation of EKAR in adult cardiac myocytes.* Myocytes expressing EKAR were detected by Cerulean fluorescence (CFP, bottom images) and treated with vehicle (Control) or angiotensin II (AngII, 100 nM) for 5 min at 25 °C. EKAR activity was recorded by FLIM and intensity images were generated with red indicating increased EKAR activity (top images) as described in detail in the Methods. C. *EKAR intensity.* EKAR intensity, corrected for photons collected, for Control (n = 22) and AngII treated myocytes (n = 22). Individual myocytes are shown, and paired groups are indicated. Average intensity for Control versus AngII treated myocytes were compared by paired (shown, Table 1) and unpaired *t*-test (Table 1).

3.4. α1-ARs, but not AT-Rs, increase bad phosphorylation, preserve mitochondrial membrane potential, and prevent cell death in adult cardiac myocytes

To determine the consequences of differential activation of ERK by α1-ARs and AT-Rs on cardiac myocyte survival, we measured survival-signaling responses in adult cardiac myocytes treated with PE and AngII. Previously, we demonstrated that ERK activation was required for α1-mediated survival signaling [14], and suggested that ERK-induced phosphorylation of Bcl-2 family members preserves

Table 1
EKAR intensity

	Control intensity ($x10^{-5}$)	Treated intensity ($x10^{-5}$)	Fold change (paired)	n	P value	Fold change (unpaired)	n	P value
Phenylephrine								
All myocytes	1.738 ± 0.042	1.833 ± 0.061	6.3 ± 3.8%	21	0.1533[a]	5.5 ± 3.5%[b]	21	0.2090[d]
Responders	1.709 ± 0.061	1.983 ± 0.064	16.8 ± 3.6%	13	0.0004[a]	15.3 ± 3.3%[c]	13	0.0005[e]
Non-responders	1.785 ± 0.052[h]	1.589 ± 0.051	−10.8 ± 2.3%	8	0.0034[a]	−10.4 ± 2.1%[c]	8	0.0015[e]
Angiotensin II								
All myocytes	1.871 ± 0.046	1.823 ± 0.052	−1.4 ± 3.5%	22	0.4684[a]	−2.6 ± 2.8%[f]	22	0.4958[d]
Responders	1.757 ± 0.079	1.992 ± 0.082	13.95 ± 3.1%	9	0.0010[a]	11.3 ± 3.5%[g]	8	0.0001[e]
Non-responders	1.950 ± 0.046[i]	1.706 ± 0.047	−12.0 ± 2.9%	13	0.0017[a]	−10.5 ± 1.7%[g]	14	0.0001[e]

[a] Paired student's *t*-test.
[b] Calculated from the average baseline in control myocytes of 1.738×10^{-5}.
[c] Determined from treated myocytes with a fold change > 1 (responders) or < 1 (non-responders) relative to the average baseline in control myocytes of 1.738×10^{-5}.
[d] Unpaired student's *t*-test.
[e] One-sample t-test for deviation from a theoretical mean of 1.0.
[f] Calculated from the average baseline in control myocytes of 1.871×10^{-5}.
[g] Determined from treated myocytes with a fold change > 1 (responders) or < 1 (non-responders) relative to the average baseline in control myocytes of 1.871×10^{-5}.
[h] Unpaired *t*-test P = 0.40 baseline PE responder vs non-responder sorted based on a paired grouping.
[i] Unpaired t-test P = 0.03 baseline AngII responder vs non-responder sorted based on a paired grouping.

mitochondrial membrane potential and prevents cell death [9]. Bad, a member of the Bcl-2 family, is downstream of α1-AR activation and phosphorylation of Bad at Ser112, a target downstream of GqPCR signaling promotes mitochondrial membrane stability [20]. Conversely, AT-R signaling is associated with increased cell death [4], conforming to the classic model of GqPCR pathologic signaling.

To measure phosphorylation of Bad, we treated myocytes with PE, AngII, or Dox, a known pro-apoptotic compound, and quantified phosphorylation of Bad at Ser112 by Western blot. PE, but not AngII or Dox, increased Bad phosphorylation at Ser112 (Fig. 4A–B). To measure mitochondrial membrane stability, we employed JC-1, a dye that is sensitive to changes in mitochondrial membrane potential. JC-1 accumulates in mitochondria and fluoresces red under normal conditions, but when mitochondria membrane potential is lost, JC-1 accumulates in the cytosol and red fluorescence decreases. We treated myocytes with PE, AngII, or Dox and quantified red fluorescence. PE, but not AngII, increased JC-1 red fluorescence (Fig. 4C–D), suggesting α1-ARs improved mitochondria membrane stability. Additionally, we assessed myocyte rod-shaped morphology, which we previously demonstrated as an index of myocyte survival [14,21]. Again, PE, but not AngII or Dox, preserved myocyte rod-shaped morphology (Fig. 4E). In summary, α1-ARs activate an ERK-dependent survival-signaling pathway to induce Bad phosphorylation, stabilization of mitochondrial membranes, and prevention of cell death, whereas, AT-Rs do not activate ERK and are associated with increased cardiac myocyte death.

4. Discussion

Here, we identified differences in GqPCR mediated activation of ERK correlated with known effects of these receptors on cardiac myocyte survival, consistent with our recently proposed model of compartmentalized GqPCR signaling in adult cardiac myocytes [15]. Using Western blots to detect ERK activation in cultured adult cardiac myocytes, we found that α1-ARs, but not AT-Rs, significantly increased phosphorylation of ERK consistent with increased ERK activity (Fig. 1). Limitations of the one-dimensional readout afforded by Western blots led us to employ a FRET-based ERK activity biosensor, EKAR, to examine ERK activity in single adult cardiac myocytes. Using EKAR to measure the compartmentalization of α1-AR and AT-R mediated ERK activity, we found that α1-ARs activated ERK at the nucleus and in the cytosol in a subset of myocytes (Fig. 2), while AT-Rs failed to show a consistent ability to activate ERK, and no nuclear AT-R induced EKAR activity was detected (Fig. 3). Quantitatively, due to limitations that prevented continuous FLIM recordings from a single myocyte, we measured agonist-induced EKAR activity from separate control and treated cells within a single dish. Using both paired and unpaired analyses to quantify EKAR activity (Table 1), we found that α1-ARs significantly increased EKAR intensity in 13/21 (62%) cardiac myocytes, in good concordance with prior reports demonstrating the α1A-subtype is expressed in only 60% of cardiac myocytes [19], whereas EKAR activity was reduced in 8/21 (38%) of myocytes, the functional significance of which is presently unclear (Fig. 2, Table 1). Conversely, we found that AT-Rs produced no significant increase in EKAR activity, and although we observed a small population of myocytes in which AT-Rs increased EKAR activity, differences in baseline EKAR intensity in responder and non-responder groups tempered this finding (Fig. 3, Table 1). Activation of ERK in cardiac myocytes is cardioprotective [22], and we found that α1-ARs, but not AT-Rs, induced phosphorylation of Bad, a member of the Bcl-2 family, stabilized mitochondrial membranes, and promoted cell survival (Fig. 4). Although AT-Rs can induce arrestin-mediated activation of ERK in some situations [23], AngII activates Gq-signaling with 10-fold greater potency than arrestin-mediated signaling [24]. Therefore, based on the observed effects on cell survival, any AngII-arrestin-mediated activation of ERK, if it occurs, did not prevent cell death. In summary, α1-ARs and AT-Rs differentially activate ERK both qualitatively, based on localization, and quantitatively, based on degree of activation and percent of responding cells, that correlates to cardiac myocyte survival.

One of the interesting outcomes we observed was that PE increased ERK activity as measured by EKAR in 13/21, or roughly 60%, of cardiac myocytes examined. Previously, using a reconstitution system to restore α1-subtype-signaling in α1ABKO cardiac myocytes that lack endogenous α1-ARs, we demonstrated that the α1A-subtype, but not the α1B, activates ERK in adult cardiac myocytes [14]. Interestingly, in α1AKO or α1BKO cardiac myocytes, we found that endogenous levels of α1-subtype expression are not sufficient to induce ERK activation [25]. While increasing α1B-subtype expression in α1AKO cardiac myocytes never restores α1-mediated activation of ERK, we observed that adding the α1B-subtype to endogenous levels of α1A-subtype in α1BKO cardiac myocytes restores α1-mediated activation of ERK [25]. These previous results suggest that the formation of α1A-α1B heterooligomers facilitate α1-mediated activation of ERK in adult cardiac myocytes [25]. Recently, it was reported that the α1A-subtype is expressed in only 60% of adult cardiac myocytes with high expression in

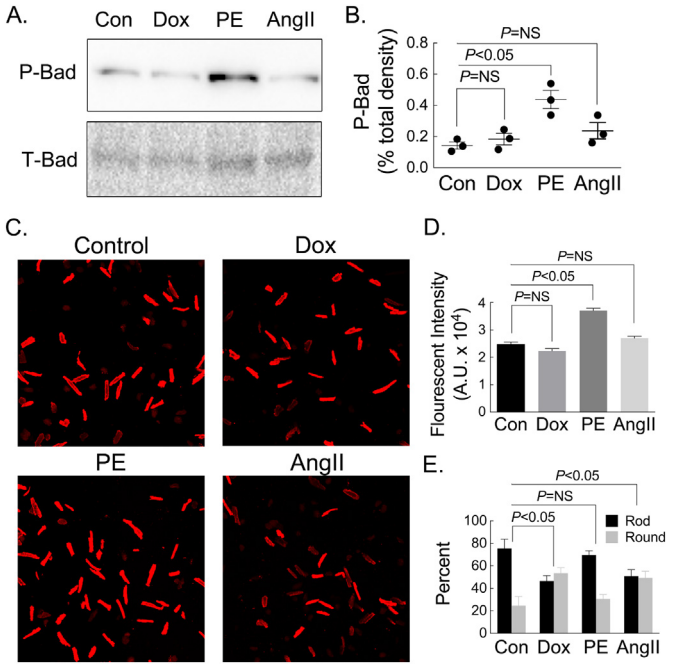

Fig. 4. α1-ARs, but not AT-Rs, increase Bad phosphorylation, preserve mitochondrial membrane potential and prevent cell death in adult cardiac myocytes.

A. *Bad Western blot.* WT AMVM were treated with vehicle (Con), doxorubicin (Dox, 2 μM), phenylephrine (PE, 20 μM), or angiotensin II (AngII, 100 nM) for 15 min. Western blots were performed with primary antibodies to phosphorylated Bad (P-Bad (S112)). B. *Quantification of Bad phosphorylation.* Densitometry presented as percent of each treatment to the total P-Bad signal for n = 3 different cultures. Data are present as Mean ± SEM, and were analyzed by one-way ANOVA ($P = 0.0071$) for a primary interaction, and with a Tukey post-test, where $P < 0.05$ was considered significant. C. *Mitochondrial membrane potential assay*. Images of myocytes treated with vehicle (Control), doxorubicin (Dox, 2 μM), phenylephrine (PE, 20 μM), or angiotensin II (AngII, 100 nM) for 2 h and subsequently loaded with JC-1. Images were collected at 10× using confocal microscopy. D, E. *Quantification of JC-1 fluorescence (D) and myocyte morphology (E).* Fluorescent intensity and rod-shaped morphology of individual cardiac myocytes was determined using FIJI for n = 4 separate experiments, measuring n = 50–200 myocytes per condition in each experiment, and average fluorescent intensity was plotted Mean ± SEM. Data were analyzed by one-way ANOVA where the P value for the primary interaction was $P < 0.001$ for JC-1 fluorescence and $P = 0.012$ for myocyte morphology, and with a Tukey post-test, where $P < 0.05$ was considered significant.

20%, whereas the β1-AR and α1B-AR are expressed in all cardiac myocytes, with the β2- and β3-ARs expressed in < 5% of cardiac myocytes [19]. Furthermore, the same report demonstrated that the α1A-subtype-specific agonist A61603 induced activation of ERK and contractile responses in only 60% of isolated cardiac myocytes, with high-level activation in 20% of myocytes. Our results show good concordance with these findings, and support the concept of heterogeneity of cardiac myocyte α1A-subtype expression and function. As previously suggested [19], this finding has specific implications for α1A-mediated cardioprotection. While it is clear that the α1A-subtype mediates survival signaling and positive inotropy that protects the heart from pathologic stress in vivo [10–13,26,27], it is currently unclear how a receptor that is expressed in only 60% of cardiac myocytes can mechanistically afford these protective effects [19]. Additionally, it is unclear what might be the functional significance of our finding that EKAR activity was reduced in 8/21, or roughly 40%, of cardiac myocytes and how that could affect α1A-mediated cardioprotection.

Traditionally, GqPCR signaling is considered maladaptive [28–30], but this model fails to account for the cardioprotective effects of α1-ARs [9,31]. However, we recently proposed an updated, novel paradigm for GqPCR function in cardiac myocytes predicated upon compartmentalization of GqPCRs [15]. Owing to the lack of validated GPCR antibodies, we used fluorescent ligands to demonstrate nuclear localization of α1-ARs, consistent with our prior reports [32], and sarcolemmal localization of AT-Rs [15]. Using the fluorescent PLCβ1 activity reporter GFP-PHD [33], we demonstrated that proximal α1-AR signaling is compartmentalized to the nucleus, whereas proximal AT-R signaling is compartmentalized to the sarcolemma, consistent with receptor localization [15]. Furthermore, nuclear α1-signaling promoted HDAC nuclear export and induced a cardioprotective hypertrophic transcriptome, whereas sarcolemmal AT-R signaling failed to promote HDAC nuclear export and induced a much smaller maladaptive transcriptome [15]. Consistent with the model of maladaptive GqPCR-signaling, AT-Rs are pro-apoptotic [4], however, again failing to conform to this model, α1-ARs prevent cardiac myocyte cell death [14]. Here, we found that activation of ERK-mediated survival signaling pathways [22] were also differentially regulated by α1-ARs and AT-Rs, where α1-ARs activated ERK at nucleus and in the cytosol and prevented cell death, but AT-Rs did neither. Therefore, we again found a correlation between receptor localization and function, with nuclear GqPCR signaling inducing a cardioprotective phenotype in support of our novel paradigm of compartmentalized GqPCR signaling in adult cardiac myocytes.

In conclusion, α1-ARs, unlike AT-Rs the prototypical GqPCR, activated ERK at the nucleus and in the cytosol in adult cardiac myocytes and induced cell survival signaling pathways marked by increased phosphorylation of Bad, improved mitochondrial membrane stability, and cardiac myocyte survival. Although α1-ARs activated ERK, we also found that activation of ERK was not observed in every cardiac myocyte, consistent with prior reports suggesting α1-ARs are expressed in only 60% of cardiac myocytes [19]. Finally, these data identify important myocyte-specific differences in GqPCR signaling consistent with our model of compartmentalized GqPCR signaling in adult cardiac myocytes.

Acknowledgements

None.

Funding

This work was supported by funds from the University of Minnesota (TDO).

Appendix A. Supplementary data

Supplementary data to this article can be found online at https://doi.org/10.1016/j.yjmcc.2018.11.020.

References

[1] J.W. Adams, Y. Sakata, M.G. Davis, V.P. Sah, Y. Wang, S.B. Liggett, K.R. Chien, J.H. Brown, G.W. Dorn 2nd, Enhanced Galphaq signaling: a common pathway mediates cardiac hypertrophy and apoptotic heart failure, Proc. Natl. Acad. Sci. U. S. A. 95 (17) (1998) 10140–10145.

[2] S.A. Akhter, L.M. Luttrell, H.A. Rockman, G. Iaccarino, R.J. Lefkowitz, W.J. Koch, Targeting the receptor-Gq interface to inhibit in vivo pressure overload myocardial hypertrophy, Science 280 (1998) 574–577.

[3] N. Wettschureck, H. Rutten, A. Zywietz, D. Gehring, T.M. Wilkie, J. Chen, K.R. Chien, S. Offermanns, Absence of pressure overload induced myocardial hypertrophy after conditional inactivation of Galphaq/Galpha11 in cardiomyocytes, Nat. Med. 7 (11) (2001) 1236–1240.

[4] K. Hasegawa, E. Iwai-Kanai, S. Sasayama, Neurohormonal regulation of myocardial cell apoptosis during the development of heart failure, J. Cell. Physiol. 186 (1) (2001) 11–18.

[5] L. Hein, M.E. Stevens, G.S. Barsh, R.E. Pratt, B.K. Kobilka, V.J. Dzau, Overexpression of angiotensin AT1 receptor transgene in the mouse myocardium produces a lethal phenotype associated with myocyte hyperplasia and heart block, Proc. Natl. Acad. Sci. U. S. A. 94 (12) (1997) 6391–6396.

[6] P. Paradis, N. Dali-Youcef, F.W. Paradis, G. Thibault, M. Nemer, Overexpression of

angiotensin II type I receptor in cardiomyocytes induces cardiac hypertrophy and remodeling, Proc. Natl. Acad. Sci. U. S. A. 97 (2) (2000) 931–936.
[7] T. Senbonmatsu, S. Ichihara, E. Price Jr., F.A. Gaffney, T. Inagami, Evidence for angiotensin II type 2 receptor-mediated cardiac myocyte enlargement during in vivo pressure overload, J. Clin. Invest. 106 (3) (2000) R25–R29.
[8] S.G. Chrysant, Angiotensin II receptor blockers in the treatment of the cardiovascular disease continuum, Clin. Ther. 30 (Pt 2) (2008) 2181–2190.
[9] T.D. O'Connell, B.C. Jensen, A.J. Baker, P.C. Simpson, Cardiac alpha1-adrenergic receptors: novel aspects of expression, signaling mechanisms, physiologic function, and clinical importance, Pharmacol. Rev. 66 (1) (2014) 308–333.
[10] J. Beak, W. Huang, J.S. Parker, S.T. Hicks, C. Patterson, P.C. Simpson, A. Ma, J. Jin, B.C. Jensen, An oral selective alpha-1A adrenergic receptor agonist prevents doxorubicin cardiotoxicity, JACC Basic Transl. Sci. 2 (1) (2017) 39–53.
[11] M.D. Montgomery, T. Chan, P.M. Swigart, B.E. Myagmar, R. Dash, P.C. Simpson, An alpha-1A adrenergic receptor agonist prevents acute doxorubicin cardiomyopathy in male mice, PLoS ONE 12 (1) (2017) e0168409.
[12] T.D. O'Connell, P.M. Swigart, M.C. Rodrigo, S. Ishizaka, S. Joho, L. Turnbull, L.H. Tecott, A.J. Baker, E. Foster, W. Grossman, P.C. Simpson, Alpha1-adrenergic receptors prevent a maladaptive cardiac response to pressure overload, J. Clin. Invest. 116 (4) (2006) 1005–1015.
[13] C.C. Yeh, Y. Fan, Y. Xu, Y.L. Yang, P.C. Simpson, M.J. Mann, Shift towards greater pathologic post-myocardial infarction remodeling with loss of the adaptive hypertrophic signaling of alpha1 adrenergic receptors in mice, PLoS ONE 12 (12) (2017) e0188471.
[14] Y. Huang, C.D. Wright, C.L. Merkwan, N.L. Baye, Q. Liang, P.C. Simpson, T.D. O'Connell, An alpha1A-adrenergic-extracellular signal-regulated kinase survival signaling pathway in cardiac myocytes, Circulation 115 (6) (2007) 763–772.
[15] E.F. Dahl, S.C. Wu, C.L. Healy, B.A. Harsch, G.C. Shearer, T.D. O'Connell, Subcellular compartmentalization of proximal Galphaq-receptor signaling produces unique hypertrophic phenotypes in adult cardiac myocytes, J. Biol. Chem. 293 (23) (2018) 8734–8749 (PMID: 29610273).
[16] C.D. Harvey, A.G. Ehrhardt, C. Cellurale, H. Zhong, R. Yasuda, R.J. Davis, K. Svoboda, A genetically encoded fluorescent sensor of ERK activity, Proc. Natl. Acad. Sci. U. S. A. 105 (49) (2008) 19264–19269.
[17] T.D. O'Connell, M.C. Rodrigo, P.C. Simpson, Isolation and culture of adult mouse cardiac myocytes, Methods Mol. Biol. 357 (2007) 271–296.
[18] S.C. Warren, A. Margineanu, D. Alibhai, D.J. Kelly, C. Talbot, Y. Alexandrov, I. Munro, M. Katan, C. Dunsby, P.M. French, Rapid global fitting of large fluorescence lifetime imaging microscopy datasets, PLoS ONE 8 (8) (2013) e70687.
[19] B.E. Myagmar, J.M. Flynn, P.M. Cowley, P.M. Swigart, M.D. Montgomery, K. Thai, D. Nair, R. Gupta, D.X. Deng, C. Hosoda, S. Melov, A.J. Baker, P.C. Simpson, Adrenergic receptors in individual ventricular myocytes: the beta-1 and alpha-1B are in all cells, the alpha-1A Is in a subpopulation, and the beta-2 and beta-3 are mostly absent, Circ. Res. 120 (7) (2017) 1103–1115.
[20] D.M. Valks, S.A. Cook, F.H. Pham, P.R. Morrison, A. Clerk, P.H. Sugden, Phenylephrine promotes phosphorylation of Bad in cardiac myocytes through the extracellular signal-regulated kinases 1/2 and protein kinase A, J. Mol. Cell. Cardiol. 34 (7) (2002) 749–763.
[21] Y. Huang, C.D. Wright, S. Kobayashi, C.L. Healy, M. Elgethun, A. Cypher, Q. Liang, T.D. O'Connell, GATA4 is a survival factor in adult cardiac myocytes but is not required for {alpha}1A-adrenergic receptor survival signaling, Am. J. Phys. 295 (2) (2008) H699–H707.
[22] C.P. Baines, J.D. Molkentin, STRESS signaling pathways that modulate cardiac myocyte apoptosis, J. Mol. Cell. Cardiol. 38 (1) (2005) 47–62.
[23] C. Oro, H. Qian, W.G. Thomas, Type 1 angiotensin receptor pharmacology: signaling beyond G proteins, Pharmacol. Ther. 113 (1) (2007) 210–226.
[24] J.D. Violin, S.M. DeWire, D. Yamashita, D.H. Rominger, L. Nguyen, K. Schiller, E.J. Whalen, M. Gowen, M.W. Lark, Selectively engaging beta-arrestins at the angiotensin II type 1 receptor reduces blood pressure and increases cardiac performance, J. Pharmacol. Exp. Ther. 335 (3) (2010) 572–579.
[25] C.D. Wright, S.C. Wu, E.F. Dahl, A.J. Sazama, T.D. O'Connell, Nuclear localization drives alpha1-adrenergic receptor oligomerization and signaling in cardiac myocytes, Cell. Signal. 24 (2012) 794–802.
[26] X.J. Du, L. Fang, X.M. Gao, H. Kiriazis, X. Feng, E. Hotchkin, A.M. Finch, H. Chaulet, R.M. Graham, Genetic enhancement of ventricular contractility protects against pressure-overload-induced cardiac dysfunction, J. Mol. Cell. Cardiol. 37 (5) (2004) 979–987.
[27] X.J. Du, X.M. Gao, H. Kiriazis, X.L. Moore, Z. Ming, Y. Su, A.M. Finch, R.A. Hannan, A.M. Dart, R.M. Graham, Transgenic alpha1A-adrenergic activation limits post-infarct ventricular remodeling and dysfunction and improves survival, Cardiovasc. Res. 71 (4) (2006) 735–743.
[28] G.W. Dorn, J.H. Brown 2nd, Gq signaling in cardiac adaptation and maladaptation, Trends Cardiovasc. Med. 9 (1–2) (1999) 26–34.
[29] N. Frey, E.N. Olson, CARDIAC HYPERTROPHY: The good, the bad, and the ugly, Annu. Rev. Physiol. 65 (2003) 45–79.
[30] Y.K. Tham, B.C. Bernardo, J.Y. Ooi, K.L. Weeks, J.R. McMullen, Pathophysiology of cardiac hypertrophy and heart failure: signaling pathways and novel therapeutic targets, Arch. Toxicol. 89 (9) (2015) 1401–1438.
[31] B.C. Jensen, T.D. O'Connell, P.C. Simpson, Alpha-1-adrenergic receptors: targets for agonist drugs to treat heart failure, J. Mol. Cell. Cardiol. 51 (2011) 518–528.
[32] C.D. Wright, Q. Chen, N.L. Baye, Y. Huang, C.L. Healy, S. Kasinathan, T.D. O'Connell, Nuclear alpha1-adrenergic receptors signal activated ERK localization to caveolae in adult cardiac myocytes, Circ. Res. 103 (9) (2008) 992–1000.
[33] T.P. Stauffer, S. Ahn, T. Meyer, Receptor-induced transient reduction in plasma membrane PtdIns(4,5)P2 concentration monitored in living cells, Curr. Biol. 8 (6) (1998) 343–346.